JOURNAL OF OPTOELECTRONICS AND ADVANCED MATERIALS Vol. 10, No. 1, January 2008, p. 44 - 54

Photonic crystals resonant cavities. Quality factors

B. LAZĂR, P. STERIAN
Bucharest Polytechnic University, Academic Center for Optical Engineering and Photonics, 77206 Bucharest, Romania

The essential property of photonic crystals, namely their capacity to forbid the propagation of electromagnetic field in all directions, leads immediately to the idea of building tiny resonant cavities having high quality factors [3-14]. Such resonators, with well controlled frequencies and life times, can be used, together with photonic guides, at the construction of various active and passive optical devices like: lasers, filters, demultiplexors, splitters, etc. In general, photonic resonators are built by introducing a defect in the perfect crystal. Usually, such inhomogeneities admit one or more resonances whose frequencies can be adjusted to fall inside one of the forbidden bands of the perfect crystal. If the cavity is surrounded by many layers, formed by elementary crystal cells, then there is no way for the field to go to and the quality factor, *Q*, tends to infinity. For walls of finite size, *Q* has limited values. What is desired are resonators as small as possible with *Q* as large as possible. The main goal of the current paper is to analyze, using FDTD (Finite Difference Time Domain) method, the structures of modes (field maps, resonant frequencies and quality factors) corresponding to some cavities, build in a photonic crystal with square symmetry.

(Received September 24, 2007; accepted January 10, 2007)

Keywords: Photonic crystal, Resonant cavity, Quality factor, Square symmetryFinite Difference Time Domain (FDTD) method

1. Introduction

For preventing the evasion of light from a certain region of space, having an arbitrary shape, that area have to be surrounded by a medium which forbids omni directionally the propagation of electromagnetic field for the frequency range of interest. Mathematical calculations [1] prove that a material having periodic electric permittivity, named also Photonic Crystal, possesses frequency gaps and in consequence the electromagnetic field in the range of prohibited bands, can not propagate.

Therefore, using such repetitive media, by simply encircling a certain part of space with periodic walls, resonant cavity can be created. These resonators are one of the most elementary photonic devices that can be build, being also constitutive elements which are used in the construction of other, more complex, active or passive micro-optical components.

2. Photonic resonators

In general a photonic resonator is built by modifying the structure of the crystal in a certain region [2]. Fig. 1 presents two examples of resonant cavities, made inside a bidimensional structure composed of circular elements which repeat along *x* and *y*. Photonic crystals have complex configurations of frequency gaps, most of them having one or two large enough forbidden spaces. In consequence the cavities must be designed in such a way to be able to admit modes with frequencies inside the crystal gaps. Simple mathematical approaches capable to determine the parameters of optical resonators, starting from a given configuration of modes, do not exist. Everything that can be done is the successive alteration of the cavity geometry till a desired result is obtained.

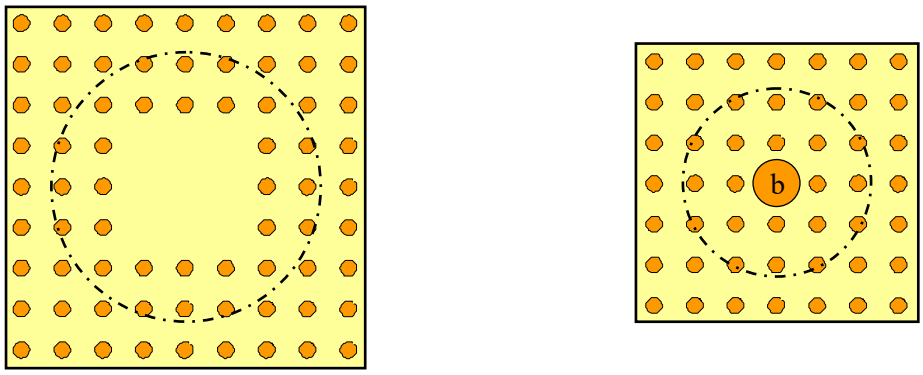

Fig. 1. Two resonant cavities. (a) The first is obtain by removing nine periodic elements, (b) the second by enlarging the diameter of a single building block.

Having a given cavity, like in Fig. 1, a possible method for studying its properties is based on the mathematical method FDTD (Finite Difference Time Domain). In essence, the resonant space is excited with a signal characterized by a flat band in a certain range of interest. In parallel the amplitude of the oscillation is recorded in one or more points inside the cavity, for an interval long enough as the resonances could be detected with satisfactory precision using the Fourier transform.

This procedure permits the examination of complicated resonators with thick walls formed by many layers of elementary cells. The field maps, corresponding to each mode, can be easily calculated and visualized. However, there are disadvantages, if the sources are placed in improper locations less modes than exist are excited. Also, an unsuitable arrangement of measuring points (in the nodes of modes) leads to signals from which some modes are absent. As nothing is a priori known about the number and geometry of the modes, numerous attempts with sources and measuring points placed in various locations have to be made in order to detect all modes.

3. Eigen frequencyes, field maps

In what follows, the resonances of the cavity in Fig. 2, formed by an inhomogeneity surrounded by three layers of periodic building blocks, will be studied. In general, the thicker the walls are the higher the quality factor of each mode is, also, the possibility of loosing resonances, due to short life time of modes, decreases considerably. The excitation source is located in a position as asymmetrical as possible in respect to the symmetry axes of the cavity, for preventing an improper placement (in a node of some mode). For increasing the detection probability of modes, two measuring points are used. The diagrams in Fig. 5 show the spectra of the signals measured in the locations [*-0.5a, 0*] and [*-0.6a, -0.6a*] respectively in respect to the center of the photonic crystal depicted in Fig. 2. The excitation source has the spectrum given in Fig. 3 and acts in the point [*0.4a, 0.6a*], where *a* is the crystal period.

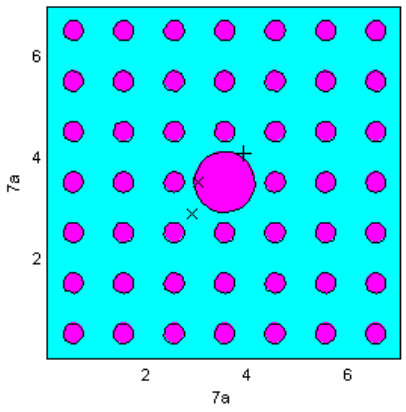

Fig. 2 Resonant cavity. The central entity has a ray, r_d=0.6a. The electric permittivity of the circularly elements are ε_{ra}= =11.56 and the background medium has ε_{rb}=1.

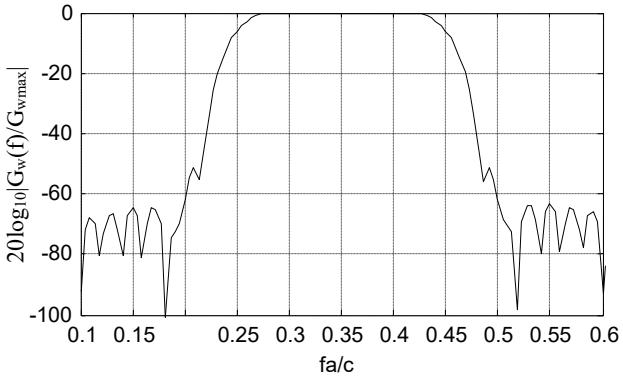

Fig. 3 The spectrum of the excitation signal that acts in the points marked with "+" in Fig. 2, Fig. 20, Fig. 21, Fig. 30.

As can be noticed from Fig. 5, the spectral component with f_n=*0.3205* is missing, so the measuring point having the coordinates [*-0.6a, 0.6a*] is placed in a null of the corresponding mode. Also, the diagram in Fig. 4 shows that the mode with f_n=*0.2987* is highly attenuated, in other words the location [*-0.5a, 0*] is in the neighborhood of a node. However, by combining the information in both diagrams, the forth modes appear in a clear way, as can be seen in Fig. 6. As a note: f_n=*fa/c*, where *f* is the real frequency, *a* the period of the crystal, *c* the speed of light in vacuum.

Once the resonances are found, the next step is the computation of the field maps corresponding to each mode. In all cases, the amplitude of the excitation is taken to be *A=2* [*a.u.*]. The field maps are displayed at moments when the lobs are clearly visible. Not every time a single source is enough for properly exciting a mode. In many instances a unique signal generator, located in a point that is not a null for a certain mode, can excite other modes leading to distortions of the field maps. In consequence, as a general rule, first of all, a singular source is moved from place to place in order the symmetry of the mode be detected. After that, for proper excitation, an assembly of sources located according to the lobs of the mode are used. The values of eigen frequencies also depends on the number of samples used for discretising the photonic structure. Thus, the same cavity has slightly different resonances when the *N* × *N* matrix that samples the cavity, changes in size. The structures in Fig. 2, Fig. 20, Fig. 21, Fig. 30 having dimensions *7a* × *7a* are sampled with *238* × *238* elements. The greater *N* × *N* is the better the precision becomes. However, a compromise has to be made, spaces sampled with exaggerated resolution leading to prohibitive calculation times.

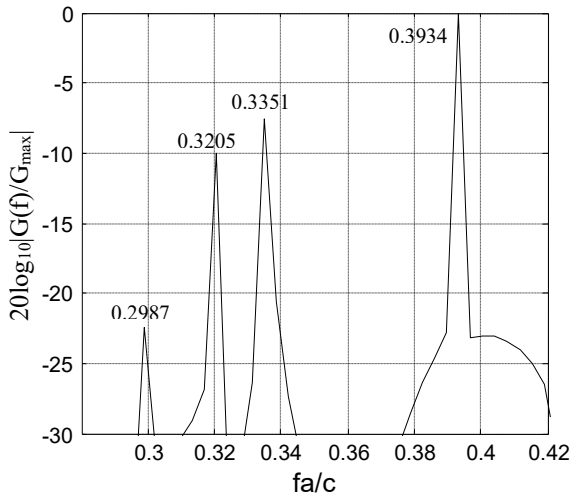

Fig. 4 The spectrum of the signal measured in [-0.5a, 0] when the source in Fig. 3 acts in [0.4a, 0.6a], (see Fig. 2).

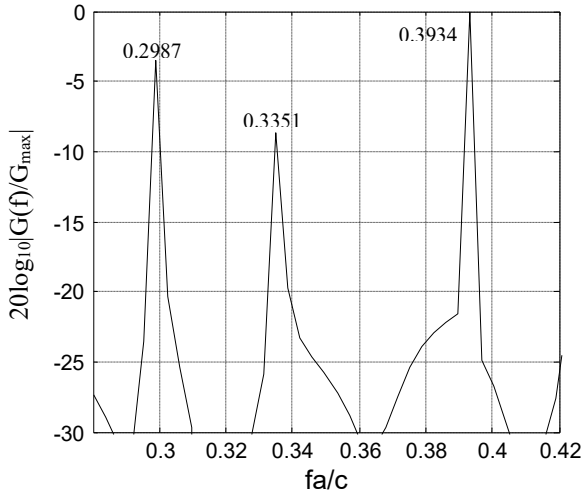

Fig. 5 The spectrum of the signal in [-0.6a, 0.6a] when the source in Fig. 3 acts in [0.4a, 0.6a], (see Fig. 2).

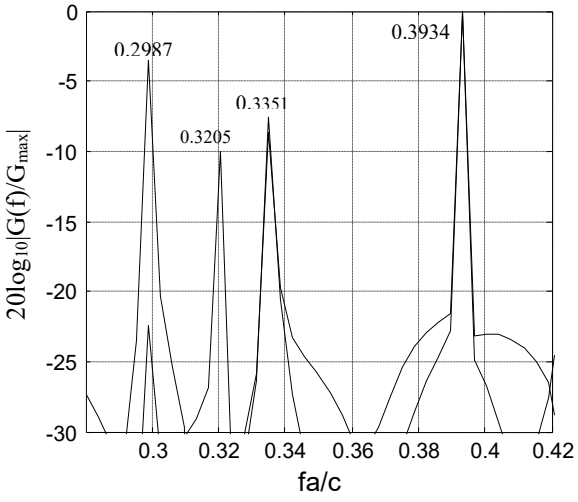

Fig. 6 The superposition of the spectra from Fig. 4 and Fig. 5.

Coming back to the particular cavity, described in Fig. 2, whose resonances are given in Fig. 6, we can display now the corresponding field maps of each detected mode. As it can be seen in Fig. 7, Fig. 8, Fig. 9, Fig. 10, the four field distributions (the component $E_z=E_z(x,y)$ at an arbitrary moment of time) have the shape of two quadrupoles, Fig. 7, Fig. 8, a monopole, Fig. 9 and a degenerated hexapol, Fig. 10. The modes are categorized as a function of number of lobs corresponding to each one. As a note, for the case illustrated in Fig. 10, a second mode along the other diagonal, can also exists for symmetry reasons. Also, as a remark, for a different placement of the excitation points corresponding to the mode four, the sum or difference of the two degenerated modes could have been excited causing the appearance of two distribution of intensity one along x and the other along y.

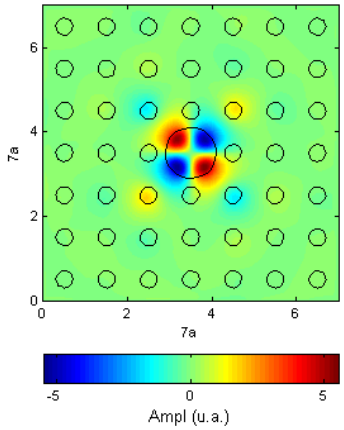

Fig. 7 The field map of the mode with f_n=0.2987 (Mod 1). Two excitation sources located in [0.4a, 0.6a], [-0.4a, -0.6a], having the expression 2sin(2πft) and another two placed in [0.4a, -0.6a], [-0.4a, 0.6a] with changed polarity, -2sin(2πft), have been used. Initially an excitation located in [0.4a, 0.6a] succeeded in activating the mode with minimal distortions.

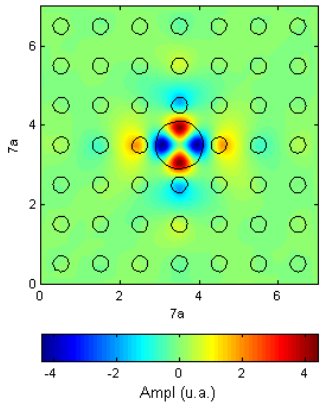

Fig. 8. The field map of the mode with f_n=0.3205 (Mod 2). Two excitation sources placed in [0, 0.7a], [0, -0.7a] having the expression 2sin(2πft) and another two located in [0.7a, 0], [-0.7a, 0] with changed polarity, -2sin(2πft), have been used. Initially a sourced positioned in [0, 0.6a] excited the mode but with distortions.

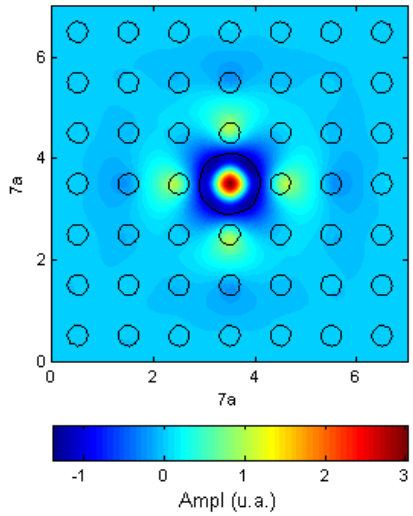

Fig. 9. The field map of the mode with f_n=0.3351 (Mod 3). A sinusoidal excitation source located in [0, 0] was used.

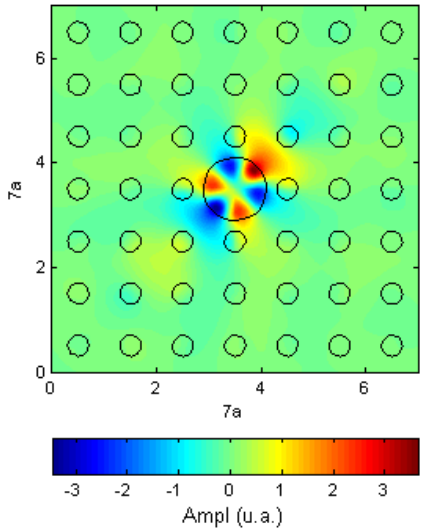

Fig. 10 The field map of the mode with f_n=0.3934 (Mod 4). Two excitation sources have been utilized: the first is located in [0.3a, 0.3a] and has the expression 2sin(2πft) and the second is placed in [-0.3a, -0.3a] having a changed polarity, -2sin(2πft). Initially, for detecting the general shape of the mode, a source located in [0.7a, 0.7a] was used.

4. Method for the evaluation of *q* using the FDTD procedeure

The four resonant modes, in the pervious paragraph, maintain their amplitude, after the source is removed, only for an ideal cavity, which means the resonator is encircled by extremely thick walls that do not have looses. If the cavity has walls, formed by a single layer of periodical elements, then the energy accumulate inside will be quickly radiated as compared to the situation when three layers thick walls surround the resonator. For a clear image of the life time corresponding to each mode, as a function of the walls width, the quality factor of the cavity needs to be evaluated.

In general the quality factor, symbolized by Q, is a physical quantity that compares the frequency a system oscillates with the rates it dissipates its energy. A high Q corresponds to a small dissipation rate as compared to the oscillation frequency. In optics the quality factor is defined as:

$$Q = \frac{2\pi f_0 \xi}{P},\ P = -\frac{d\xi}{dt}, \tag{1}$$

where f_0 is the mode frequency and ξ the energy in the cavity.

Solving the equation (1), in respect to ξ, the following solution is obtained:

$$\xi(t) = \xi(0) e^{-2\pi f_0 \frac{t}{Q}} \tag{2}$$

If the energy in the resonator is known, at two different moments of time: t_1 and t_2, then using (2), Q takes the form:

$$\frac{\xi(t_1)}{\xi(t_2)} = e^{\frac{2\pi f_0}{Q}(t_2 - t_1)} \Rightarrow Q = \frac{2\pi f_0 (t_2 - t_1)}{\ln(\xi(t_1)/\xi(t_2))}. \tag{3}$$

The fraction $\xi(t_1)/\xi(t_2)$ can not be easily calculated. In what follows, a more simple relation, equivalent to $\xi(t_1)/\xi(t_2)$, will be deduced starting from Maxwell equations (1)-(4):

$$(1)\ \nabla \times \mathbf{E} = -\frac{\partial \mathbf{B}}{\partial t},\ (2)\ \nabla \cdot \mathbf{B} = 0,\ (3)\ \nabla \times \mathbf{H} = \frac{\partial \mathbf{D}}{\partial t} + \mathbf{j}(\mathbf{r},t),$$
$$(4)\ \nabla \cdot \mathbf{D} = \rho(\mathbf{r},t), \tag{4}$$

where

$$\mathbf{D} = \varepsilon \mathbf{E} = \varepsilon_0 \varepsilon_r \mathbf{E},\quad \mathbf{H} = \frac{\mathbf{B}}{\mu} = \frac{\mathbf{B}}{\mu_0 \mu_r},\ \mathbf{j}(\mathbf{r},t) = 0,\quad \rho(\mathbf{r},t) = 0 \tag{5}$$

and

$$\mu_r = 1,\ \varepsilon_r = \varepsilon_r(\mathbf{r}). \tag{6}$$

If the expressions (4) - (1) and (3) are multiplied by **H** and **E,** respectively, and (3) is subtracted from (1), the following theorem is obtained:

$$\nabla \cdot (\mathbf{E} \times \mathbf{H}) = -\varepsilon \mathbf{E} \frac{\partial \mathbf{E}}{\partial t} - \mu \mathbf{H} \frac{\partial \mathbf{H}}{\partial t} = -\frac{\partial}{\partial t} \underbrace{\left(\frac{1}{2} \varepsilon \mathbf{E}^2 + \frac{1}{2} \mu \mathbf{H}^2 \right)}_{\text{Energy density}}$$

(Poynting's theorem) (7)

For deducing the formula (7), the identity: $\nabla \cdot (\mathbf{E} \times \mathbf{H}) = \mathbf{H} \nabla \times \mathbf{E} - \mathbf{E} \nabla \times \mathbf{H}$ was used, where **E** and **H** are two arbitrary vectors. By using the relation:

$$\mathbf{B} = \frac{1}{c} \mathbf{n} \times \mathbf{E}, \tag{8}$$

where **n** is an unitary vector perpendicular to **E**, it can be immediately proven that the two components of the energy density: magnetic and electric, from (8), are equal to each other:

$$\frac{1}{2}\mu\mathbf{H}^2 = \frac{\mathbf{B}^2}{2\mu} = \frac{1}{2\mu}\frac{1}{c^2}(\mathbf{n}\times\mathbf{E})^2 = \frac{1}{2}\varepsilon\mathbf{E}^2 . \quad (9)$$

In consequence, the total density of energy is:

$$\frac{1}{2}\varepsilon\mathbf{E}^2 + \frac{1}{2}\mu\mathbf{H}^2 = \varepsilon\mathbf{E}^2 \quad (10)$$

or:

$$\xi = \int_V \varepsilon\mathbf{E}^2 dv . \quad (11)$$

For the cavities studied in this paper the field is supposed to have the particular form:

$$E(x,y,t) = E(x,y)f(t)e^{j\omega_r t} , \quad (12)$$

where ω_r is the resonant pulsation and $f(t)$ a damping function with the amplitude $E(x,y)$.
With the help of (11), (12), the fraction $\xi(t_1)/\xi(t_2)$, from (3), takes the form:

$$\frac{\xi(t_1)}{\xi(t_2)} = \frac{\int_S \varepsilon_0\varepsilon_r(x,y)E^2(x,y)f^2(t_1)\sin^2\omega_r t_1 ds}{\int_S \varepsilon_0\varepsilon_r(x,y)E^2(x,y)f^2(t_2)\sin^2\omega_r t_2 ds} = \left(\frac{f(t_1)\sin\omega_r t_1}{f(t_2)\sin\omega_r t_2}\right)^2 \quad (13)$$

where $f(t_1)/f(t_2)$ is evaluated using the expression:

$$\frac{f(t_1)}{f(t_2)} = \frac{E_m(x_m,y_m)(t_1)}{E_m(x_m,y_m)(t_2)} \quad (14)$$

$E_m(x_m,y_m)(t_{1,2})$ are the instantaneous values of the signal in the resonant cavity, measured at the same location: (x_m, y_m), at two distinct moments t_1 and t_2.

Therefore, the expression of Q from (3) turns in:

$$Q = \frac{\pi f_r(t_2 - t_1)}{\ln\left(\frac{E_m(x_m,y_m)(t_1)}{E_m(x_m,y_m)(t_2)}\frac{\sin 2\pi f_r t_1}{\sin 2\pi f_r t_2}\right)} \quad (15)$$

where f_0 is renamed as f_r (resonance frequency).

In conclusion, the quality factor is evaluated using elements that can be easily calculated using the FDTD method. The electric field amplitudes, measured in the same location at two different moments of time, are much more simple to be obtained as compared with the total energy inside the resonator at the same moments.

Therefore, using (15), the value of Q factor corresponding to all four modes of the resonator in Fig. 2 can be evaluated, for various thickness of its walls. Modes with small Q, that oscillate inside cavities with thin walls (a single layer of periodic cells), tend quickly to zero and in consequence the FDTD algorithm, that calculates the amplitudes in the cavity as a function of time, does not have to be run for long periods. For high Qs the amplitude of the signal in the resonator decreases slowly, staying nearly constant for relatively long intervals.

5. Numerical evaluation of *Q* for a few resonant cavities

In the current paragraph, using the theory developed in the previous one, some Q factors, corresponding to particular resonant cavities, will be calculated. First of all, the quality factors of the modes from Fig. 7 – Fig. 10 are estimated. The results are presented in Fig. 11 - Fig. 19 and centralized in Table 1.

R=0.6, Mod1

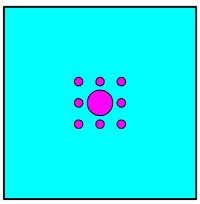

Q=131.3

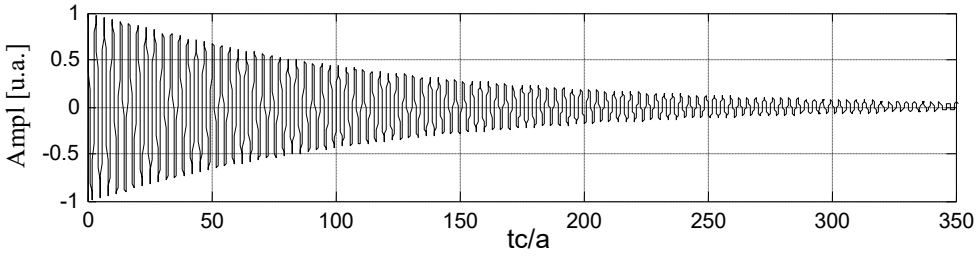

Fig. 11 E_m(0.4a, 0.6a)(13.5963)=0.9052; E_m(0.4a, 0.6a)(293.2155)=0.0811 → Q=131.3.

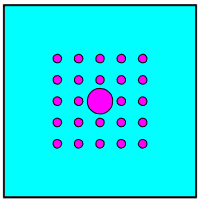

Q=1080

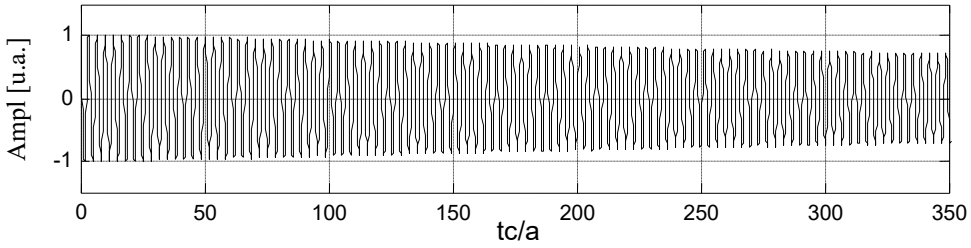

Fig. 12 E_m(0.4a, 0.6a)(57.0626)=0.963; E_m(0.4a, 0.6a)(291.9676)=0.7527 → Q=1080.

R=0.6, Mod2

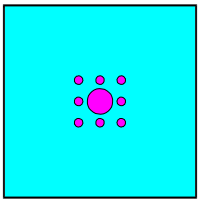

Q=38.8

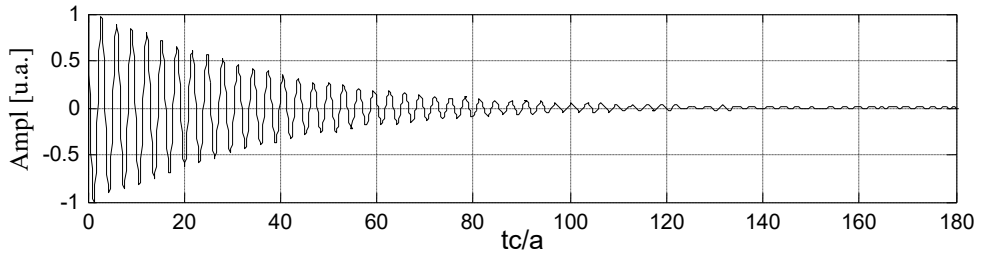

Fig. 13 $E_m(0, 0.6a)(9.1769)=0.8454$; $E_m(0, 0.6a)(65.7454)=0.1621 \rightarrow Q=38.8$.

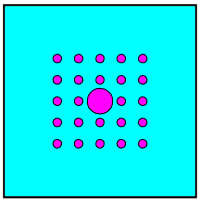

Q=345.4

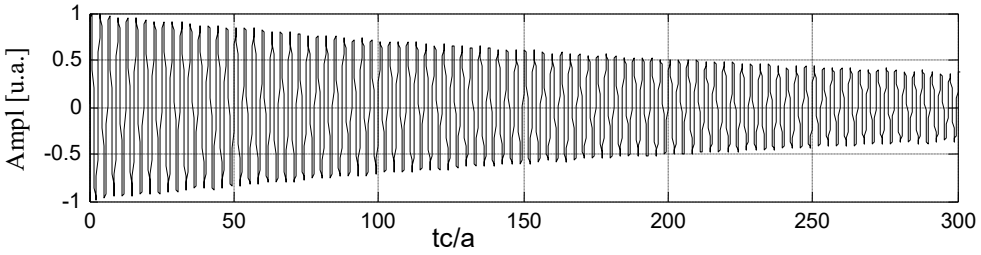

Fig. 14 $E_m(0, 0.6a)(110.113)=0.6982$; $E_m(0, 0.6a)(275.6592)=0.4057 \rightarrow Q=345.4$.

R=0.6, Mod3

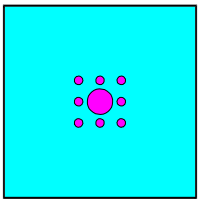

Q=59.1

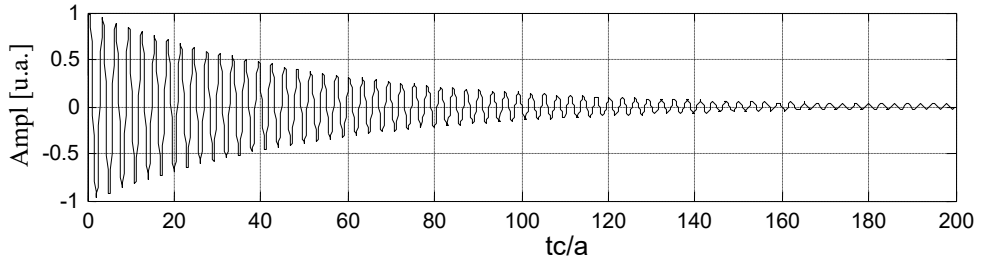

Fig. 15 $E_m(0, 0)(18.5356)=0.7098$; $E_m(0, 0)(123.2498)=0.0954 \rightarrow Q=59.1$.

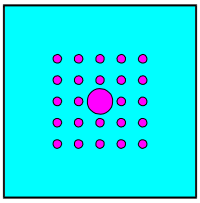

Q=549.6

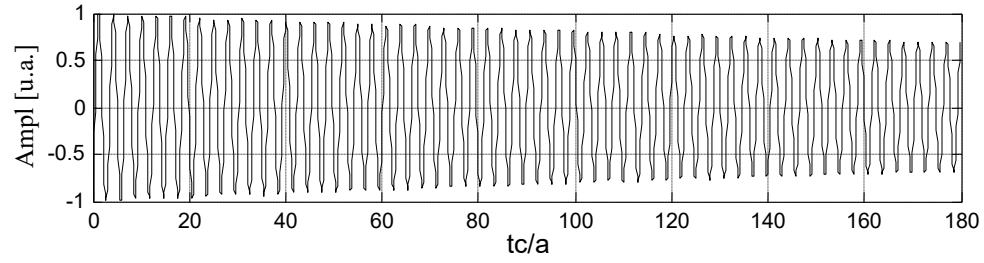

Fig. 16 $E_m(0, 0)(34.0989)=0.9341$; $E_m(0, 0)(159.1944)=0.7218 \rightarrow Q=549.6$.

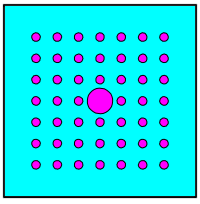

Q=5349

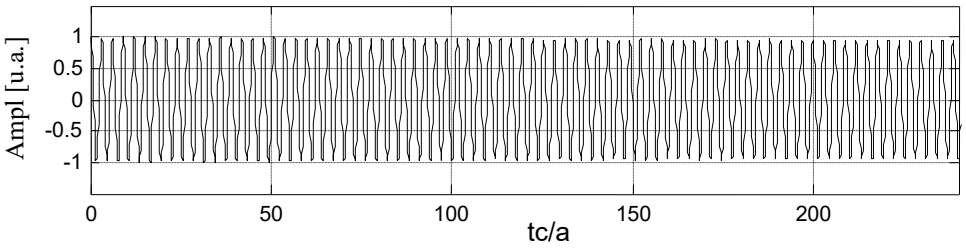

Fig. 17 $E_m(0, 0)(18.0677)=0.9928$; $E_m(0, 0)(223.6486)=0.9505 \rightarrow Q=5349$.

R=0.6, Mod4

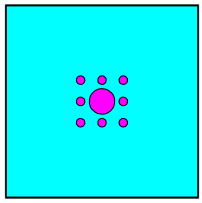

Q=412.7

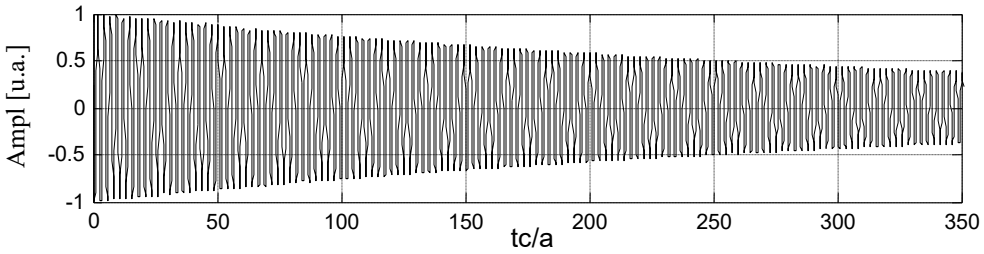

Fig. 18 E_m(0.3a, 0.3a)(164.7924)=0.6352; E_m(0.3a, 0.3a)(322.4356)=0.4121 → Q=412.7.

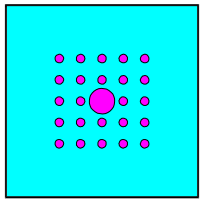

Q=4026

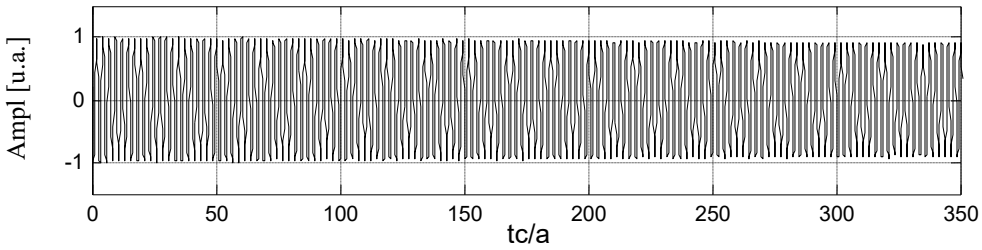

Fig. 19 E_m(0.3a, 0.3a)(207.9467)=0.9416; E_m(0.3a, 0.3a)(330.0266)=0.9098 → Q=4026.

Fig. 11 - Fig. 19 show clear images of the physical aspect of the resonators and the temporal diagrams that display the loss of amplitude as a function of time, for each mode. As a note, the moments the amplitude is calculated at, have factionary values because they are chosen in such a way that the two sin function in (15) be of unitary values. As can be remarked, the time *t* on the *x* axis was multiplied by *c/a* (where *c* is the speed of light in vacuum and *a* is the period of the crystal) in order the diagrams be read no matter the real size of the elementary cell is.

Table 1. The quality factors of the cavity in Fig. 2 for various thickness of its walls.

R=0.6	1 layer	2 layers	3 layers
Q Mod 1 – quadrupole	131.3	1080	
Q Mod 2 – quadrupole	38.8	345.4	
Q Mod 3 – monopole	59.1	549.6	5349
Q Mod 4 – hexapole	412.7	4026	

The data in Table 1 show considerable variations of the quality factors. The highest *Q* belongs to the hexapole and the smallest to the quadrupole 2 followed at sort distance by the monopole.

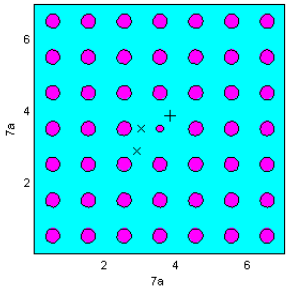

Fig. 20 Resonant cavity. The central entity has a ray, r_d=0.1a. The electric permittivity of the circular elements are ε_{ra} =11.56 and that of the background medium is, ε_{rb}=1.

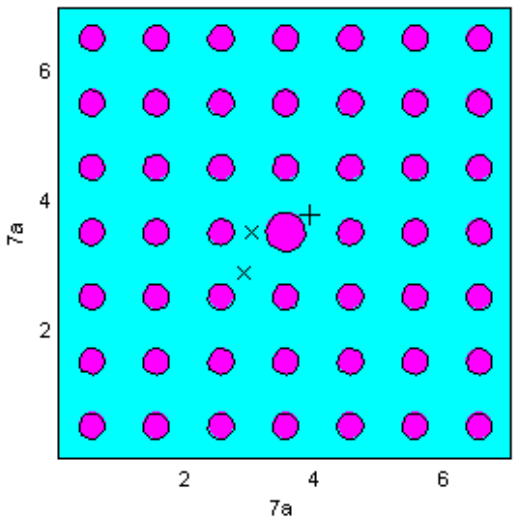

Fig. 21 Resonant cavity. The central entity has a ray, r_d=0.3a. The electric permittivity of the circular elements are ε_{ra} =11.56 and that of the background medium is, ε_{rb}=1.

The main conclusion, resulting from Table 1, is the exponential growth of *Q* as the walls of the resonators increase in width. All four modes show an order of magnitude raise for each added layer of elementary cells. This fact indicates that very small resonators with high quality factors can be build using photonic crystals.

Using the same procedure as for the cavity characterized by an impurity with *r=0.6*, another three resonators with dopant elements having smaller diameters, will be studied (see Figs. 20, 21 and Fig. 30).

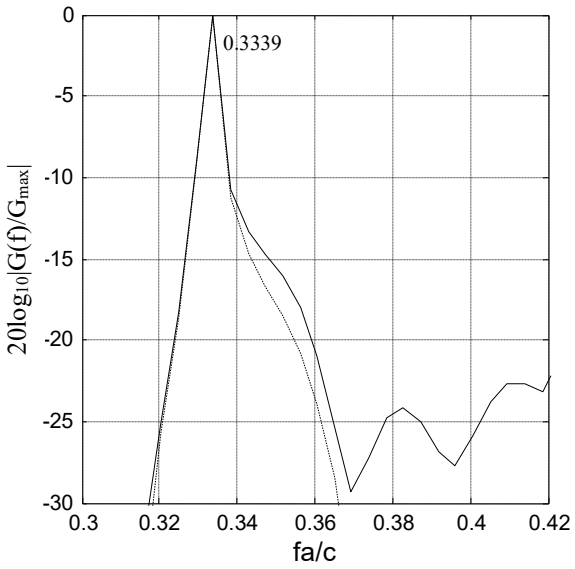

Fig. 22. The spectra of the signals measured in: [-0.5a, 0] – dashed line and [-0.6a, -0.6a] – solid line, when the source from Fig. 3 acts in [0.4a, 0.3a]. (see Fig. 20).

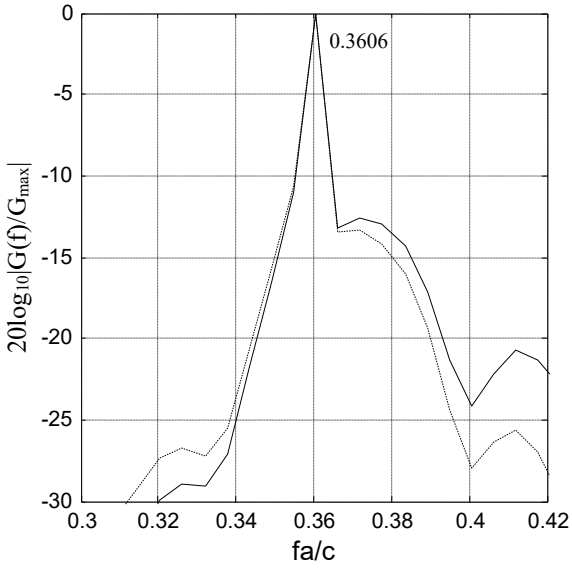

Fig. 23. The spectra of the signals measured in: [-0.5a, 0] – dashed line and [-0.6a, -0.6a] – solid line, when the source in Fig. 3 acts in [0.4a, 0.3a]. (see Fig. 21).

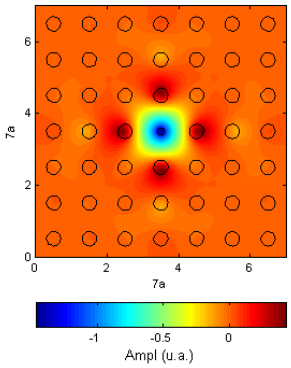

Fig. 24 The field map of the mode with f_n=0.3339 corresponding to r_d=0.1a. A sinusoidal excitation source located in [0, 0] is used.

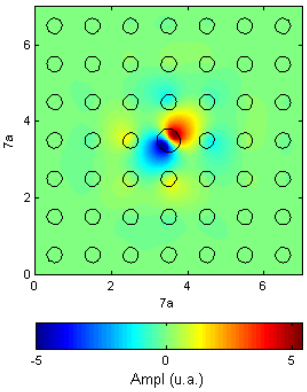

Fig. 25 The field map of the mode with f_n=0.3606 corresponding to an impurity having r_d=0.3a. Two excitation sources have been utilized: the first is placed in the point [0.3a, 0.3a] and has the time dependence 2sin(2πft) and the second in [-0.3a, -0.3a] with changed polarity, -2sin(2πft). Initially, for detecting the rough form of the mode, a source positioned in [0.4a, 0.4a] was used.

This time, all the three cavities (see Figs 24, 25 and Fig. 32) are monomode. Two of them admit monopoles and one (*r=0.3*) a degenerated dipole.

Following the same procedure as for the situation of the cavity characterized by four modes, the precise resonant frequencies (see Fig. 22, Fig. 23, Fig. 31) and the field maps corresponding to each mode (Fig. 24, Fig. 25, Fig. 32) are determined. Finally, with the help of (15), the quality factors are evaluated.

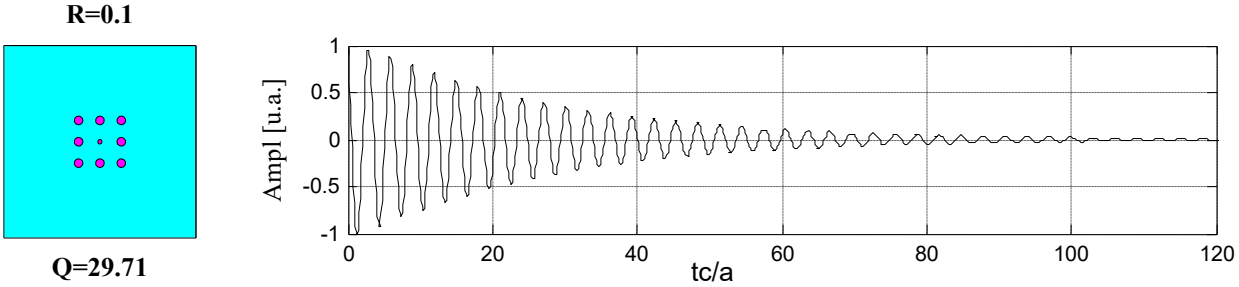

Fig. 26 E_m(0, 0)(8.8995)=0.7927; E_m(0, 0)(54.4455)=0.1396 → Q=29.71.

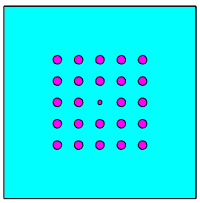

Q=283.95

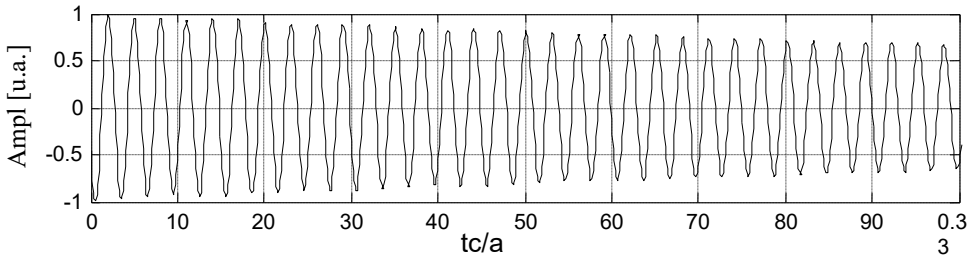

Fig. 27 $E_m(0, 0)(32.1232)=0.8782$; $E_m(0, 0)(95.2429)=0.6827 \rightarrow Q=283.95$.

R=0.3

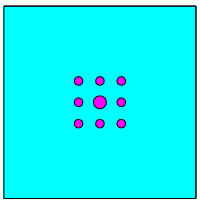

Q=54.68

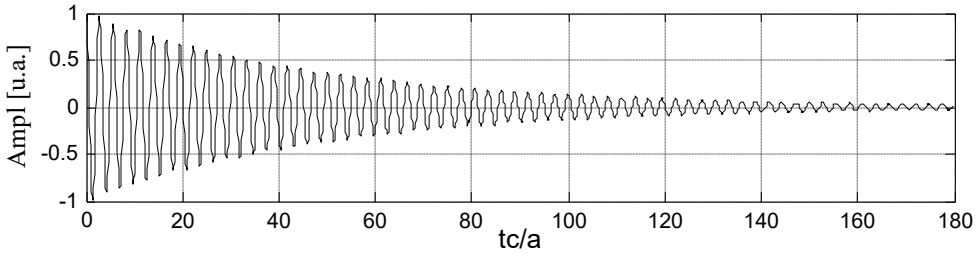

Fig. 28 E_m(0.4a, 0.4a)(11.118)=0.8114; E_m(0.4a, 0.4a)(97.2186)=0.1363 → Q=54.68.

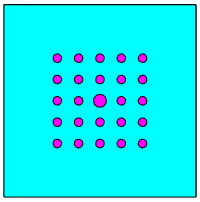

Q=555.32

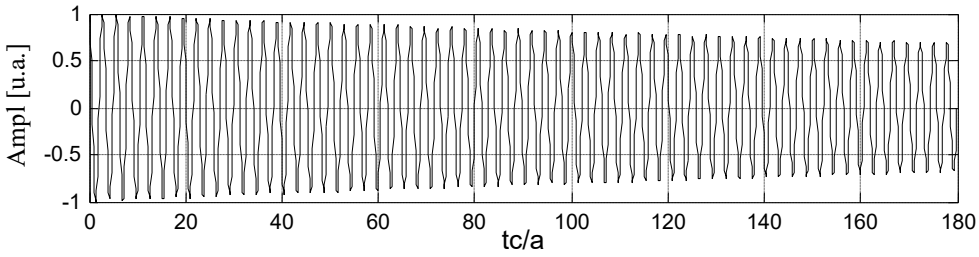

Fig. 29 $E_m(0.4a, 0.4a)(47.3052)=0.895$; $E_m(0.4a, 0.4a)(175.1043)=0.6896 \rightarrow Q=555.32$.

Table 2. The quality factors of the cavity in Fig. 20 for two widths of its walls.

R=0.1	1 layer	2 layers
Q Mod - monopole	29.71	283.95

Table 3. *The quality factors of the cavity in Fig. 21 for two widths of its walls.*

R=0.3	1 layer	2 layers
Q Mod - dipole	54.68	555.32

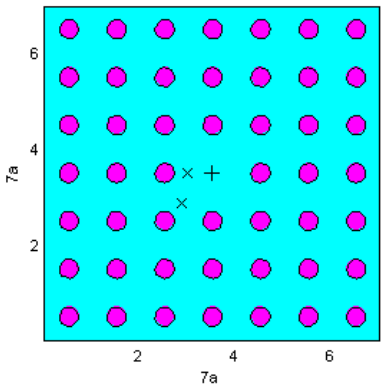

Fig. 30 Resonant cavity. The permittivity of the circular elements is $\varepsilon_{ra}=11.56$ and that of the background medium is $\varepsilon_{rb}=1$.

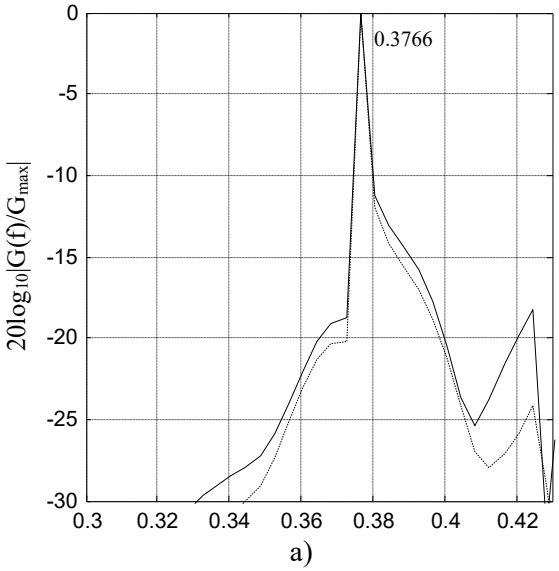

Fig. 31 The spectra of the signals measured in: [-0.5a, 0] – dashed line and [-0.6a, -0.6a] – solid line, when the source in Fig. 3 acts in [0, 0]. (see Fig. 30).

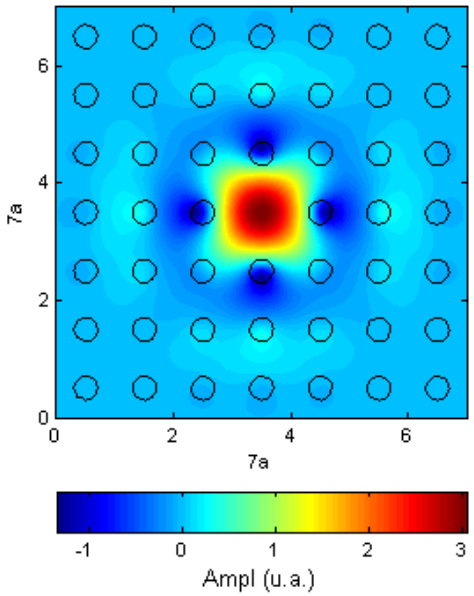

Fig. 32 The field map of the mode with f_n=0.3766 corresponding to an impurity having r_d=0. A sinusoidal excitation source located in [0, 0] was used.

Table 4. The quality factors of the cavity in Fig. 30 for three widths of its walls.

R=0	1 layer	2 layers	3 layers
Q Mod - monopole	17.46	172.73	1214

R=0

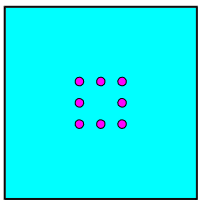

Q=17.46

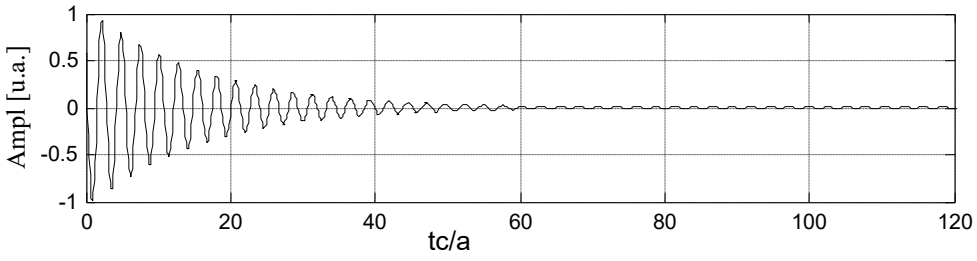

Fig. 33 $E_m(0, 0)(2.2444)=0.9304$; $E_m(0, 0)(41.8632)=0.0712 \rightarrow Q=17.46$.

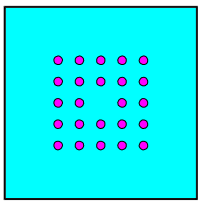

Q=172.73

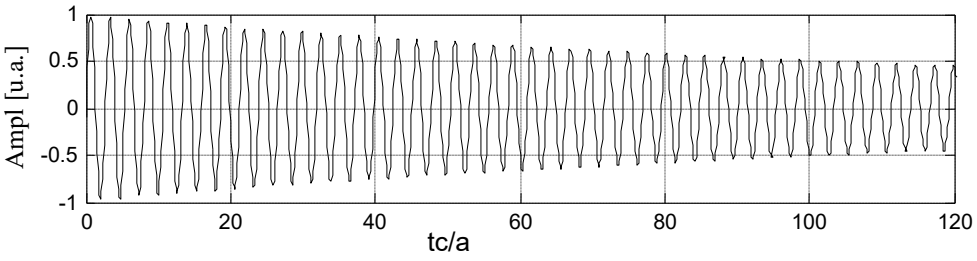

Fig. 34 $E_m(0, 0)(8.6569)=0.9298$; $E_m(0, 0)(117.3226)=0.4559 \rightarrow Q=172.73$.

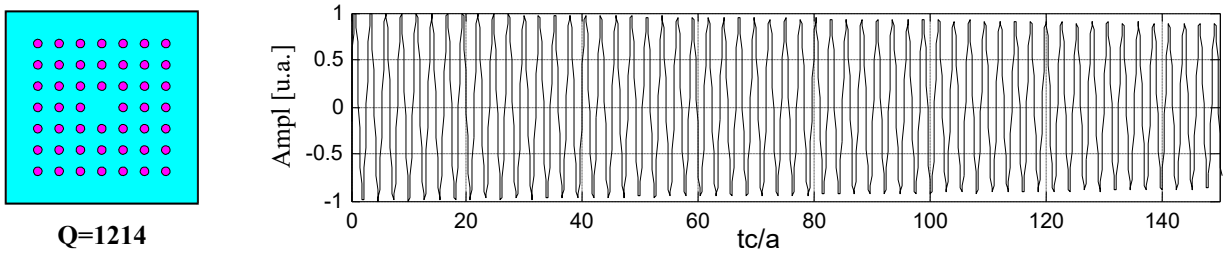

Fig. 35 $E_m(0, 0)(8.6569)=0.9992$; $E_m(0, 0)(146.6467)=0.8785 \rightarrow Q=1214$.

6. Conclusions

Despite the fact the FDTD method can give precise frequencies of resonant modes, however, without a priori data about the behavior of a particular resonator, i.e. the number of supported modes and their symmetry, this finite difference method can easily miss modes either due to putting the excitation source in an improper position or placing the measuring points in wrong locations (nodes).

After the modes frequencies are precisely established, the correspondent field maps can be calculated using FDTD. Some modes, especially the monopoles, do not need special precautions in placing the excitation source. Others, the ones having nodes: dipoles, quadrupoles, hexapoles are extremely sensible to the excitation position. For such cases, the field maps are obtained by following a procedure in two steps: (a) Firstly, a single source with the frequency of the mode and located in an asymmetrical position related to the geometry of the cavity, is used. Most likely this source will excite the mode in an improper way. (b) Once the symmetry of the mode is roughly established, two – four excitators placed in the mode lobs, having the proper polarity, are utilized. Thus, a stable, clear, and well shaped modal field is obtained. Ideally, the perfect stimulation should be done with a source having the same frequency and intensity distribution than that of the mode.

The next step consists in determining another important characteristic of resonators, namely, the quality factor. In this paper, a relatively simple formula that calculates Q starting from the evolution in time of the amplitude in one point inside the cavity, was deduced. In short, each mode have been excited, for different widths of the walls that surround the cavity. After that, the source or sources were removed and the field in the cavity was left to freely oscillate. From the temporal diagram of the decreasing amplitude in one point of the resonator, using the formula we talked previously, the quality factor Q is calculated.

Two important remarks have to be made:

a) The life time of modes varies strongly from one to the other. For instance, the monopole corresponding to the resonator with impurity ray $r=0.6$ has a life time almost ten time shorter than the hexapol.

b) In average, independently of the mode, the quality factors grow an order of magnitude for each supplemental layer of elementary cells added to the width of the wall.

References

[1] K. M. Ho, C. T. Chan, C. M. Soukoulis, Physical Review Letters **65**(25), 3152 (1990).
[2] G. Guida, P. N. Stavrinou, G. Parry, J. B. Pendry, Journal Of Modern Optics **48**(4), 581 (2001).
[3] Tomoyuki Yoshie, Jelena Vuckovic, Axel Scherer, Applied Physics Letters **79**(26), 4289 (2001).
[4] Anne-Laure Fehrembach, Stefan Enoch, Anne Sentenac, Applied Physics Letters **79**(26), 4280 (2001).
[5] Ziyang Zhang, Min Qiu, Optics Express **12**(17), 3988 (2004).
[6] N. Malkova, S. Kim, T. DiLazaro, V. Gopalan, Physical Review **B 67**, 125203 (2003).
[7] Oskar Painter, Kartik Srinivasan, John D O'Brien, J. Opt. A: Pure Appl. Opt. **3**, S161 (2001).
[8] Han-Youl Ryu, Se-Heon Kim, Hong-Gyu Park, Yong-Hee Lee, Journal of Applied Physics **93**(2), 831 (2003).
[9] Steven G. Johnson, Shanhui Fan, Attila Mekis, J. D. Joannopoulos, Applied Physics Letters **78**(22), 3388 (2001).
[10] Lazăr Bogdan, Paul Sterian, International Conference Micro to Nano Photonics, Romopto 2006, Aug. 28-31, Sibiu Romania. To be published in SPIE Proc.
[11] Dirk Englund, Jelena Vuckovic, Optics Express, **14**(8), 3472 (2006).
[12] Jelena Vuckovic, Marko Loncar, Hideo Mabuchi, Axel Scherer, IEEE Journal Of Quantum Electronics **38**(7), 850 (2002).
[13] Takashi Asano, Bong-Shik Song, Susumu Noda, Optics Express **14**(5), 1996 (2006).
[14] Yosef M. Landobasa, Mee K. Chin, Optics Express **13** (20), 7800 (2005).

*Corresponding author: sterian@physics.pub.ro